Note Added in Proof. While the series of substituted diphenylacetylenes reported in this paper exhibit centrosymmetric crystal phases (from acetonitrile solution) and are essentially SHG inactive, we[31] and others[35] have recently shown that highly SHG active (efficiencies up to 200 times urea) derivatives, e.g., NH_2, CO_2CH_3, CH_3S, and NO_2, of diphenylacetylenes can be prepared.

Registry No. I, 1211-40-1; II, 7431-22-3; III, 110175-15-0; IV, 110175-16-1; Cu(C≡CC_6H_4-p-NO_2), 123207-77-2; p-iodoaniline, 540-37-4; (p-nitrophenyl)acetylene, 937-31-5; (p-aminophenyl)acetylene, 14235-81-5; (triethylsilyl)acetylene, 1777-03-3, 7642-33-3.

Supplementary Material Available: Tables of anisotropic displacement factors (4 pages); observed and calculated structure factors (35 pages). Ordering information is given on any current masthead page.

Characterization of (Methylcyclopentadienyl)trimethylplatinum and Low-Temperature Organometallic Chemical Vapor Deposition of Platinum Metal

Ziling Xue,[†] M. Jane Strouse,[†] David K. Shuh,[†] Carolyn B. Knobler,[†] Herbert D. Kaesz,*[,†] Robert F. Hicks,[‡] and R. Stanley Williams[†]

Contribution from the Department of Chemistry and Biochemistry, University of California, Los Angeles, California 90024-1569, and Department of Chemical Engineering, University of California, Los Angeles, California 90024-1592. *Received March 6, 1989*

Abstract: (η^5-Methylcyclopentadienyl)trimethylplatinum, (η^5-MeCp)$PtMe_3$, **1** (MeCp = $CH_3C_5H_4$), is synthesized from trimethylplatinum iodide and sodium methylcyclopentadienide by the method of Fritz and Schwarzhans. By using some care in the purification of bis(methylcyclopentadiene) from dicyclopentadiene, a sample of **1** is obtained showing a melting point of 29.5–30.0 °C and a vapor pressure of 0.053 Torr at 23 °C. ^1H and ^{13}C NMR spectra have been obtained, the latter both in solution as well as in the solid state. Coupling constants to the cyclopentadienyl ring carbons are found to differ, Hz: $^{195}Pt-^{13}C_{Me}$ = 13.62, while $^{195}Pt-^{13}C_H$ = 2.82 or 5.34. Five separate resonances are observed for the ring carbon atoms of the MeCp group in the solid state $\{^1H\}^{13}C$ NMR. However, only one signal is observed at −73 °C or higher for the three methyl groups on Pt, indicating a low barrier for rotation of these groups in the solid state. The structure has been determined on a single crystal of **1** at −143 °C: monoclinic, space group $P2_1$, with a = 7.159 (2) Å, b = 11.092 (3) Å, c = 6.004 (1) Å, and β = 106.806 (6)°. The structure was solved and refined by using 907 observed ($I > 3\sigma(I)$) independent reflections measured on a Picker automated diffractometer. Refinement uncorrected for absorption converged at R = 0.034 and R_w = 0.060. The principal finding, of significance to the solid-state NMR, is the intermolecular contacts of 3.98, 4.55, and 4.94 Å between closest ring-carbon atoms on independent molecules in adjacent unit cells. These contacts are too close to permit rotation of the MeCp rings. The ring is pentahapto-bonded with almost identical Pt to ring-carbon distances within the limited accuracy of this determination, Å: $C_{(Me)}-Pt$ = 2.266, $C_{(H)}-Pt$ = 2.260, 2.314, 2.354, and 2.324. For deposition of metallic platinum, a stream of Ar gas at ambient pressure is first saturated with the vapor of **1** at 23 °C. This is then conducted into a chamber containing H_2 gas such that the ratio of saturated Ar:H_2 = 4:1. A substrate such as a glass slide or a Si(100) wafer, placed near the outlet of the saturated Ar gas stream and heated to 120 °C, becomes coated with a film of highly reflective Pt metal. The films have been characterized by powder X-ray diffraction (indicating a crystalline nature) and with X-ray photoelectron spectroscopy (XPS). A high purity, i.e., less than 1 atom % C, is indicated.

Thin films of platinum are used extensively in microelectronics device processing[1,2] and electrodeless metal plating.[3] Thermal deposition of platinum from the vapor phase has been reported with use of $Pt(acetylacetonate)_2$, $Pt(PF_3)_4$, or $Pt(CO)_2Cl_2$.[4-6] These depositions require high temperature (200–600 °C), and the films are contaminated by heteroatoms from the ligands. We have been interested in finding other volatile organometallic compounds to obtain platinum films of higher purity. The ready decomposition of tris(ethylene)platinum was already known.[7] However, this hydrocarbon precursor is much too unstable for long-range storage and handling. Recently our group[8] and others[9] have reported organometallic chemical vapor deposition (OMCVD) from hydrocarbon precursors. In our work,[8] platinum films of high purity (>99 atom %) and high crystal quality were obtained at 180 °C from $CpPtMe_3$ (Cp = cyclopentadienyl) in the presence of H_2. The need to have a liquid organometallic precursor for better control of evaporation has led us to investigate (methylcyclopentadienyl)trimethylplatinum, $(MeCp)PtMe_3$, reported[10] to be an oily substance at room temperature. Here we report our studies on this complex. A preliminary account of a part of this work has appeared.[11]

Experimental Section and Results

Preparation of $(MeCp)PtMe_3$, 1. Commercially available bis(methylcyclopentadiene) (Aldrich) is only 95% pure. The dimer is thermally

[†] Department of Chemistry and Biochemistry.
[‡] Department of Chemical Engineering.

(1) Green, M. L.; Levy, R. A. *J. Metals* **1985**, *37*, 63–71.
(2) Ghate, P. B. In *Thin Films and Interfaces*; Materials Research Society Symposium Proceedings, Ho, P. S., Tu, K. N., Eds.; Elsevier: New York, 1982; Vol. 10, pp 371–395.
(3) Bindra, P.; Roldan, J. *J. Electrochem. Soc.* **1985**, *132*, 2581–2589.
(4) Rand, M. J. *J. Electrochem. Soc.* **1973**, *120*, 686–693.
(5) Rand, M. J. *J. Electrochem. Soc.* **1975**, *122*, 811–815.
(6) Morabito, J. M.; Rand, M. J. *Thin Solid Films* **1974**, *22*, 293–303.
(7) Green, M.; Howard, J. A. K.; Spencer, J. L.; Stone, F. G. A. *J. Chem. Soc., Dalton Trans.* **1977**, 271–277.
(8) Chen, Y.-J.; Kaesz, H. D.; Thridandam, H.; Hicks, R. F. *Appl. Phys. Lett.* **1988**, *53*, 1591–1592.
(9) Gozum, J. E.; Pollina, D. M.; Jensen, J. A.; Girolami, G. S. *J. Am. Chem. Soc.* **1988**, *110*, 2688–2689.
(10) Fritz, H. P.; Schwarzhans, K.-E. *J. Organomet. Chem.* **1966**, *5*, 181–184.
(11) Kaesz, H. D.; Williams, R. S.; Hicks, R. F.; Chen, Y.-J.; Xue, Z.; Xu, D.; Shuh, D. K.; Thridandam, H. In *Chemical Perspectives of Microelectronic Materials*; Materials Research Society Symposium Proceedings, Gross, M. E., Jasinski, J. M., Yates, Jr., J. T., Eds.; Materials Research Society: Pittsburgh, PA, 1989; Vol. 131, pp 395–400.

0002-7863/89/1511-8779$01.50/0

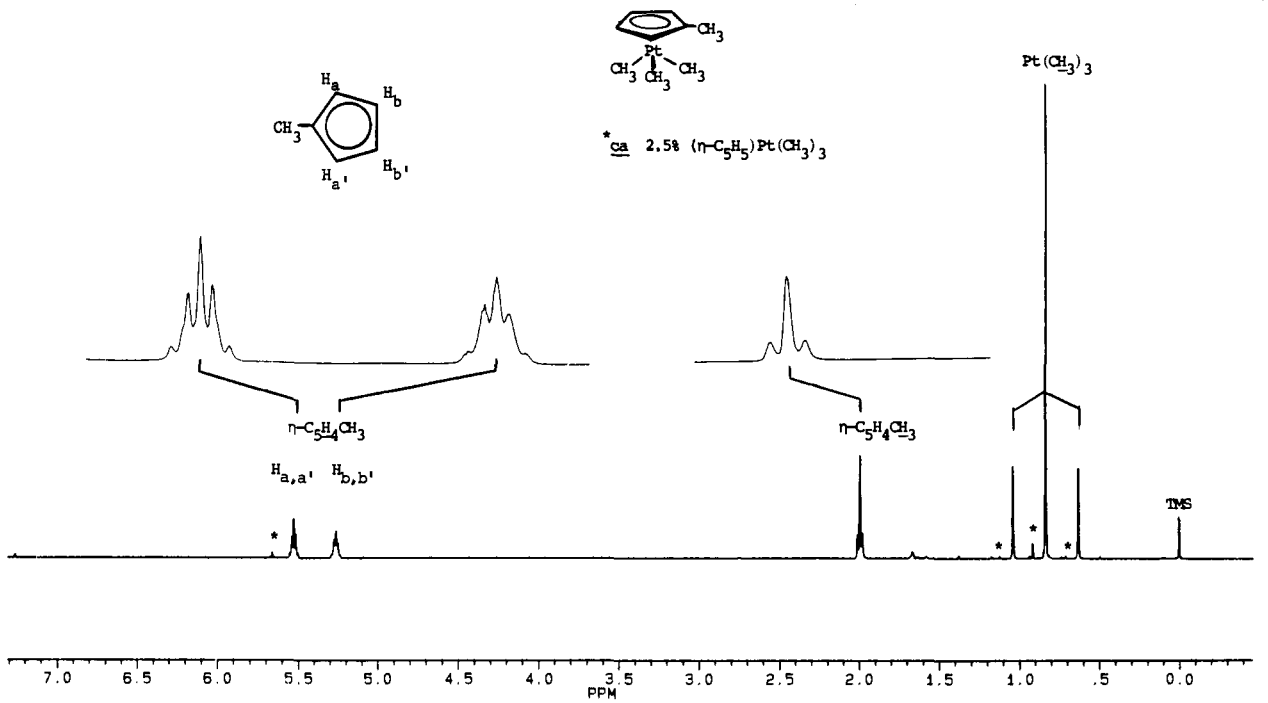

Figure 1. ^1H NMR (200.133 MHz) of **1** at 23 °C, $CDCl_3$ solution, δ(ppm) 0.83 (s, Pt-CH_3, 9 H, $J^{195}Pt-^1H$ = 81.6 Hz), 1.99 (s, $CH_3C_5H_4$, 3 H, $J^{195}Pt-^1H$ = 6.22 Hz), 5.26 ($H_{b,b'}$) and 5.52 ($H_{a,a'}$) (m, C_5H_4, 4 H, assignment based on ^1H homonuclear COSY, see Supplementary Material Figure A).

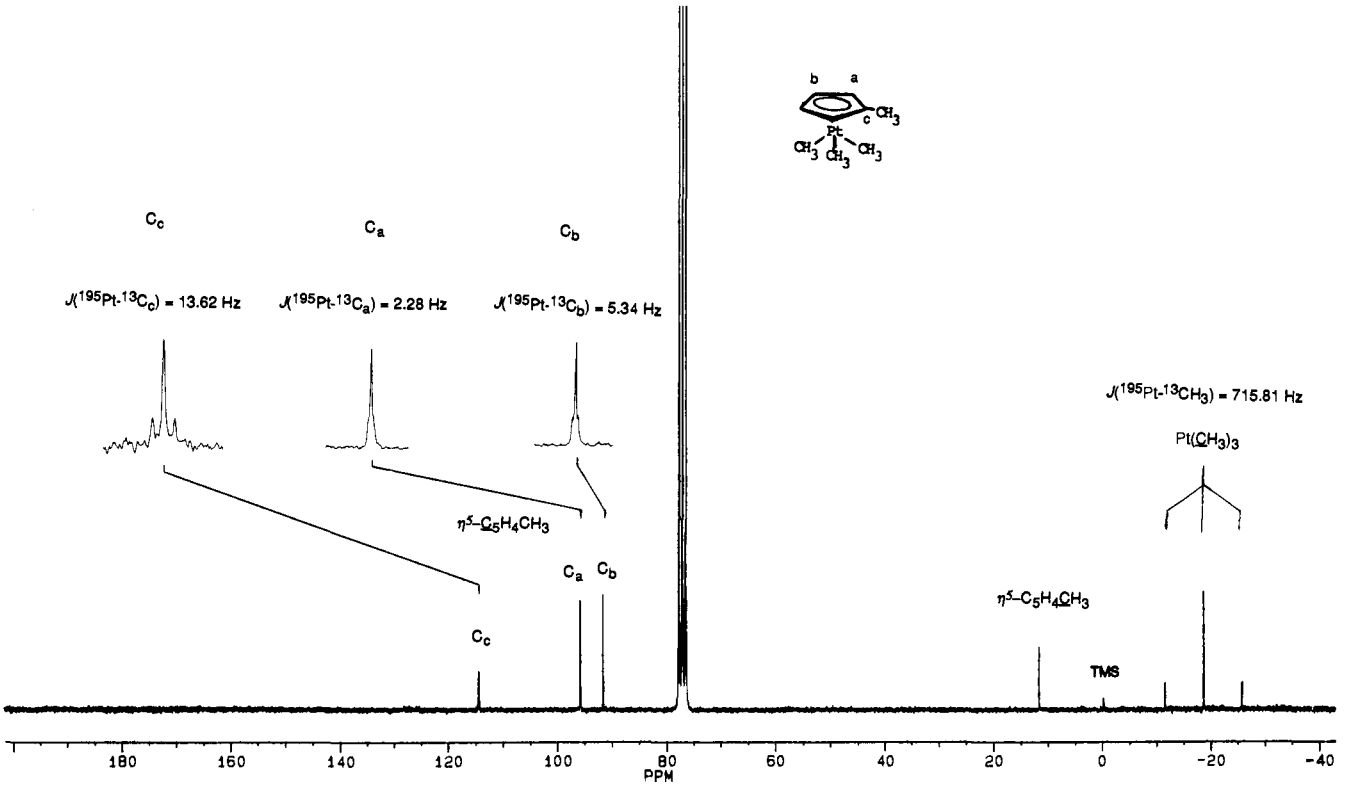

Figure 2. $\{^1H\}^{13}C$ NMR (50.323 MHz) of **1** at 23 °C, $CDCl_3$ solution, δ(ppm) −18.4 (Pt-CH_3, $J^{195}Pt-^{13}C$ = 715.81 Hz), 11.8 ($C_5H_4CH_3$), 91.8 ($C_{b,b'}$), 95.9 ($C_{a,a'}$), and 114.5 (C_c) ($C_5H_4CH_3$, assignment based on $^1H-^{13}C$ heteronuclear shift correlation, see Supplementary Material Figure B, $J^{195}Pt-^{13}C_b$ = 5.34 Hz, $J^{195}Pt-^{13}C_a$ = 2.28 Hz, $J^{195}Pt-^{13}C_c$ = 13.62 Hz).

cracked to the monomer immediately before use. During the thermal cracking, all distillate collected below the expected boiling range of methylcyclopentadiene (72.8–73.2 °C) is discarded; the desired fraction is collected in a receiver cooled to −78 °C. For larger scale preparations, the methylcyclopentadiene is redistilled.[12] This is converted to Na(MeCp) by reaction with sodium metal in tetrahydofuran (THF)[13] and is then reacted with Me_3PtI.[10] The product is purified by sublimation giving white crystals; melting point 29.5–30.0 °C. ^1H NMR (Bruker AF200) is shown in Figure 1; this indicates the presence of 2.5% of $CpPtMe_3$. Resublimation of the product makes **1** over 99.9% pure. Assignment of the resonances of the ring protons was determined through the use of ^1H two-dimensional correlation spectroscopy (COSY) on a

(12) Rettig, M. F.; Drago, R. S. *J. Am. Chem. Soc.* **1969**, *91*, 1361–1370.

(13) King, R. B.; Stone, F. G. A. *Inorg. Synth.* **1963**, *7*, 99–101.

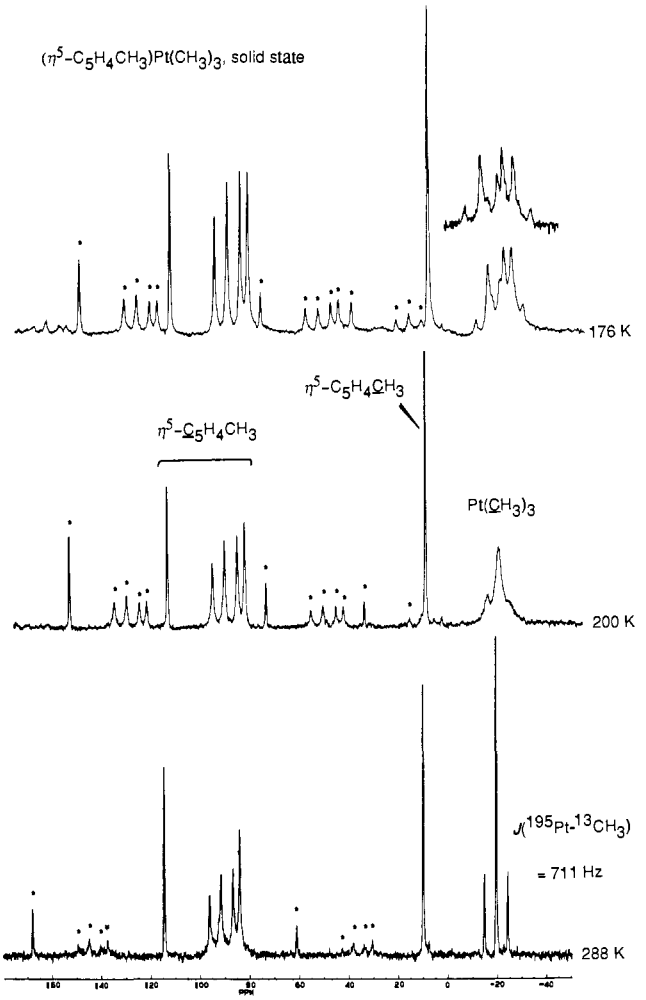

Figure 3. Solid-state $\{^1H\}^{13}C$ NMR (75.470 MHz) of **1** at 288, 200, and 176 K. Spinning side bands are indicated by an asterisk. The chemical shifts were independently determined with use of glycine carbonyl at 176.03 ppm as reference. The insert above the $Pt(\underline{C}H_3)_3$ signal in the top spectrum was obtained by resolution enhancement prior to Fourier transformation of the data; three principal resonances are observed accompanied by ^{195}Pt–^{13}C satellites (coupling constants J: ca. 710 Hz).

Bruker AF200, see Supplementary Material Figure A. Solution $\{^1H\}^{13}C$ NMR spectra (Bruker AF200) are shown in Figure 2. The resonances of the ring carbons were assigned through ^1H–^{13}C two-dimensional heteronuclear shift correlation (Bruker AF200), see Supplementary Material Figure B. Solid-state $\{^1H\}^{13}C$ NMR spectra in Figure 3 were taken at 288, 200, and 176 K on a Bruker MSL300 spectrometer with a double air bearing magic angle spinning probe. The bearing gas was nitrogen cooled by a liquid nitrogen bath. The spinning gas was nitrogen at room temperature. The temperatures reported are those of a thermocouple located in the bearing gas near the rotor.

Vapor Pressure Measurement. This was achieved by the gas-saturation method[14a] with use of the apparatus shown in Supplementary Material Figure C. Purified Ar gas is first saturated with the sample vapor by slowly passing it through a 7-mm column of the sample held on a fritted disc (14-mm diameter). Separate study[25] shows that saturation is achieved up to a flow rate of 20 mL/min; a flow rate of 8 mL/min was used in this work. The saturated gas is then passed through a heptane solution cooled to −78 °C, in which the sample is removed from the gas. The Ar gas is then slowly bubbled through excess carbon tetrachloride held at 23 °C in a gas-saturator (vapor pressure = 100 Torr);[14b] the volume of inert gas is determined by loss of weight of CCl_4. The concentrations of the complexes dissolved in the heptane solutions were determined by UV spectroscopy on a Beckman UV 5270 spectrometer: for $CpPtMe_3$, λ_{max} = 254.4 nm (cf. λ_{max} = 254 nm, $\epsilon = 1.07 \times 10^4$ and λ = 289 nm, $\epsilon = 2.19 \times 10^3$ in cyclohexane[15]); for **1**, λ_{max} = 255.4 nm (see Supplementary Material Figure D; cf. spectrum recorded in dioxane[10]). The absorptions for $CpPtMe_3$ and **1** were independently calibrated against sample concentration, see Supplementary Material Figures E and F. The volumetric flasks and the UV cells used for the calibration were thoroughly rinsed first by methanol and then by heptane. The average values of vapor pressures at 23 °C thus measured are 0.044 Torr for $CpPtMe_3$ and 0.053 Torr for **1**.

Table 1. Crystal and Intensity Collection Data for $(MeCp)PtMe_3$[a]

formula	$C_9H_{16}Pt$
formula wt.	319.31
space group	$P2_1$
a, Å	7.159 (2)
b, Å	11.092 (3)
c, Å	6.004 (1)
β, deg	106.806 (6)
V, Å^3	456.400
Z	2
ρ_{calcd} g cm^{-3}	2.32
crystal size, mm^3	0.32 × 0.32 × 0.24
scan rate, deg min^{-1}	3.0
2θ limits, deg	$0 \le 2\theta \le 50$
observations	$+h,+k,\pm l$
total obsd data	955
unique reflcns ($I > 3\sigma(I)$)	907
final no. variables	36
goodness of fit[b]	2.75
R[c]	0.034
R_w[d]	0.060

[a] Radiation source, Mo Kα = 0.71070 Å; temperature = −143 °C. [b] GOF = $[\sum w(|F_o| - |F_c|)^2/(N_o - N_v)]^{1/2}$, where $w = 1/(\sigma^2|F_o|)$. [c] $R = \sum||F_o| - |F_c||/|F_o|$. [d] $R_w = [\sum w(|F_o| - |F_c|)^2/\sum w|F_o|^2]^{1/2}$.

Single-Crystal X-ray Diffraction. Air and X-ray stable single crystals of **1** were grown by slow cooling of a liquid sample from 40 °C to −25 °C over a period of 2 days. Working in a cold room (5 °C) one crystal was glued to the tip of a glass fiber with epoxy cement. This was then mounted and centered at −143 °C on a Picker four-circle automated diffractometer equipped with a scintillation counter and a graphite-monochromator, modified at University of California, Los Angeles by Prof. C. E. Strouse for operation under control of a VAX 11/750 computer.

The 2θ, ω, χ, and ϕ settings of the Mo Kα peaks of 27 reflections (2θ = 10–20°) were determined. These values were used in a least-squares refinement of cell and orientation parameters. The refined unit cell parameters and specifics relating to collection and refinement of data are given in Table 1. The intensities of three standard reflections, (2,2,−1), (−2,−2,1), (−1,1,2), were recorded after every 97 intensity measurements throughout the data collection to monitor crystal and diffractometer stability. No decay in the intensities of the standards was observed during the 15.9 h of data collection. Reflections having $I > 3\sigma(I)$ (907) were corrected for Lorentz and polarization effects and converted to $|F_o|$ and $\sigma(|F_o|)$.[16] Indexing of the faces was difficult due to the epoxy covering on the crystal. An absorption correction was attempted based on the ψ scan procedure; however, this caused the R factors to increase and was judged unsuitable.

All calculations were performed on a VAX 11/750 computer (Department of Chemistry and Biochemistry, University of California, Los Angeles). Programs used for the structure determination consist in all cases of local modifications by Prof. C. E. Strouse and his research group.[16] Scattering factors for neutral platinum and carbon atoms were taken from Table 2.2A of ref 17. Both real (f') and imaginary (f'') components of anomalous dispersion were included for platinum using the values in Table 2.3.1 of ref 17. The function minimized during least-squares refinement and the discrepancy indices are given in Table 1.

(14) (a) Thomson, G. W.; Douslin, D. R. In *Techniques of Chemistry; Physical Methods of Chemistry*; Weissberger, A., Rossiter, B. W., Eds.; Wiley: New York, 1971; Vol. I, part 5, pp 23–104. (b) *CRC Handbook of Chemistry and Physics*, 69th ed.; Weast, R. C., Ed.; CRC Press Inc.: Boca Raton, FL, 1988–1989; p D-196.

(15) Hackelberg, O.; Wojcicki, A. *Inorg. Chim. Acta* **1980**, *44*, L63–L64.

(16) Functions and programs employed are given as follows: (a) Data reduction, Strouse, C. E. Modification of the original program written by Broach, R. W. (University of Wisconsin); Coppens, P.; Becker, P.; Blessing, R. H. (State University of New York, Buffalo). (b) Patterson and Fourier programs, adapted from algorithms in MULTAN78, Main P. (University of York, England). (c) Full-matrix least-squares and error analysis, ORFLS and ORFFE, Busing, W. R.; Martin, K. O.; Levy, H. A. (Oak Ridge National Laboratory). (d) Least-squares planes, MGTL, Gantzel, P.; Trueblood, K. N. (e) Thermal ellipsoid plot program, ORTEP II, Johnson, C. K. (Oak Ridge National Laboratory). (f) Structure factor table listing, PUBLIST, Hoel, E.

(17) *International Tables for X-ray Crystallography*; Kynoch Press: Birmingham, England, 1975; Vol. IV.

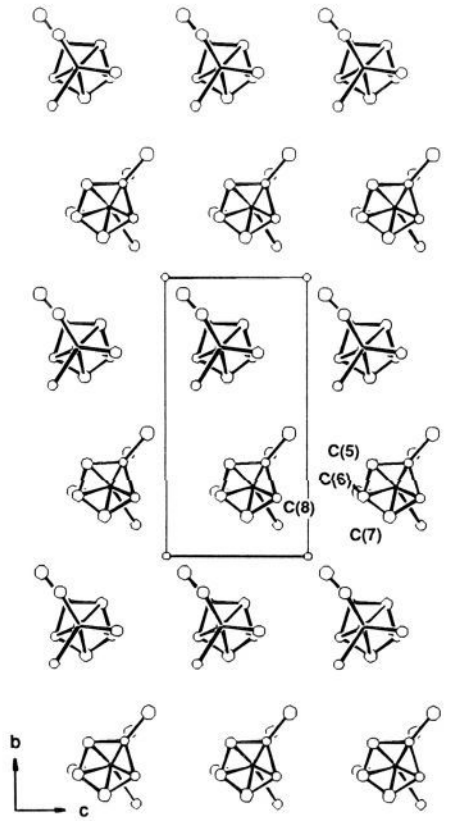

Figure 4. Packing diagram for a unit cell of **1** (the contours represent 50% of the electron density); intermolecular contacts (Å): C(8)–C(5′) = 4.55; C(8)–C(6′) = 3.98; C(8)–C(7′) = 4.94.

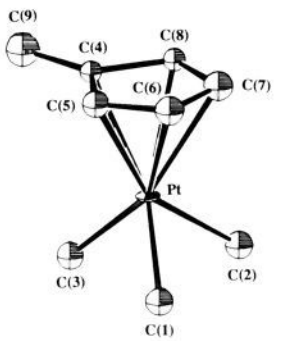

Figure 5. ORTEP projection with atom-labeling scheme for **1**; the contours represent 50% of the electron density. Hydrogen atoms are omitted for clarity.

Reasonable position parameters for the metal atom were obtained by the Patterson method. Full-matrix least-squares refinement of these parameters and an isotropic temperature factor for the metal followed by difference Fourier syntheses revealed the positions of all carbon atoms. Five carbons and four hydrogens on the Cp ring were treated as a rigid group (Å: C–C = 1.395, C–H = 0.95). At least one hydrogen atom on each of the four methyl groups was located. With use of these positions, the other hydrogen atoms on these methyl groups were fixed in calculated positions with C–H = 1.00 Å and H–C–H = 109.5°. Neither the positions nor the temperature factors were refined for the hydrogen atoms. These parameters, however, were used in the calculation of the final structure factors. Least-squares refinement with anisotropic thermal parameters for platinum afforded R factors shown in Table I and confirmed the assignment of the noncentrosymmetric space group $P2_1$. The final atomic positions are given in Supplementary Material Table B. Selected interatomic distances and angles are given in Supplementary Material Tables C and D, respectively. The final thermal parameters for the platinum are given in Supplementary Material Table E. A packing diagram of the unit cell is shown as Figure 4. The molecular structure and labeling of the atoms in $(MeCp)PtMe_3$, **1**, is shown in Figure 5. The intermolecular contacts indicated in the caption to Figure 4 are too close to permit rotation of the MeCp ring, a point to note in reference to the solid-state NMR spectra discussed below.

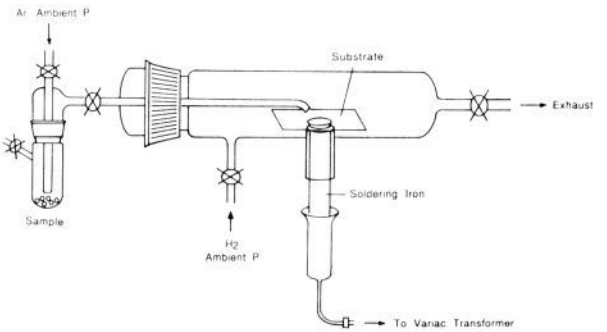

Figure 6. Diagram of the reactor for chemical vapor deposition under atmospheric pressure.

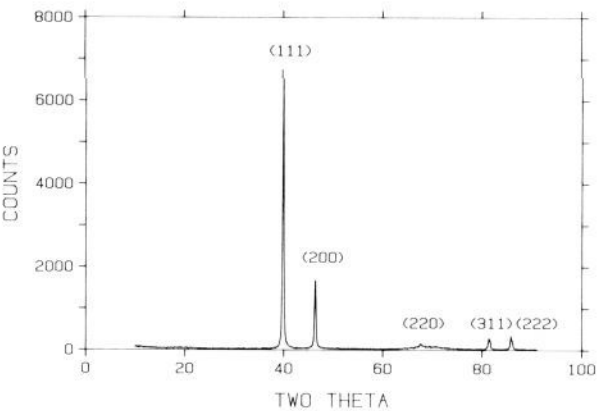

Figure 7. X-ray powder diffraction pattern of the Pt film.

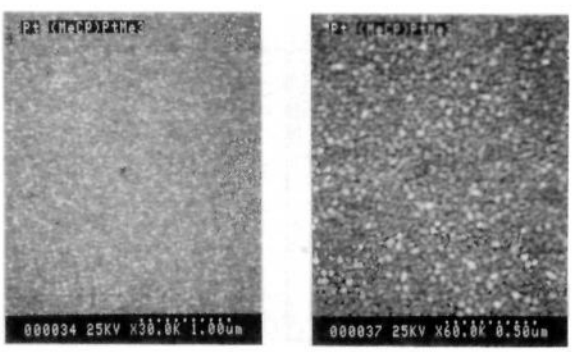

Figure 8. Scanning electron microscope (SEM) photographs of the Pt film.

Low-Temperature Chemical Vapor Deposition. This was conducted at ambient pressure in a cold-wall glass reactor shown in Figure 6. The compound is vaporized at atmospheric pressure in a stream of Ar at 23 °C and transported into the reactor at ~20 mL/min. Through a separate gas inlet, H_2 is introduced into the reactor chamber at a rate 20% that of the Ar flow. Bright and reflective Pt films are deposited on glass slides or on oriented Si(100) substrates (13.6–18.0 ohm cm, p-type) mounted on a resistively heated pedestal. The Pyrex glass slides were cleaned with acetone and deionized water prior to use. The silicon wafers were cut into pieces between 7 and 10 mm on each side and then cleaned by the following method. The wafers were first degreased in successive washes with tetrachloroethylene, acetone, and methanol. This was followed by a rinse with deionized water. Holding the wafers with plastic tweezers, they were next dipped in 10% hydrofluoric acid for 10 s, followed by a 5-min rinse in a flow of deionized water. The Si wafer was placed with polished side up on the glass heating finger of the deposition apparatus (Figure 6). Deposition of Pt from **1** occurs at the rate of about 0.2 Å/s on Si(100) at 120 °C, which is faster than the rate of 0.1 Å/s for the deposition from $CpPtMe_3$ on Si(100) at 180 °C.[8] Powder X-ray diffraction patterns of the films are shown in Figure 7; these were obtained with Cu radiation (Kα, λ = 1.5418 Å) on an automated diffractometer equipped with a scintillation counter, graphite-monochromator,

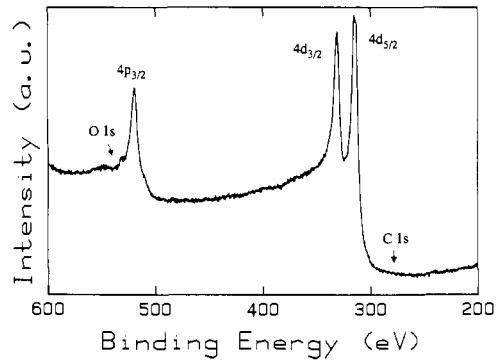

Figure 9. X-ray photoelectron spectrum of the Pt film.

modified at University of California, Los Angeles by Prof. C. E. Strouse for operation under control of a VAX 11/750 computer. Scanning electron microscopy (SEM) of the Pt film shown in Figure 8 was obtained on a Hitachi S-800 field emission scanning electron microscope (FESEM). Film resistivity was measured with the standard four-probe method.

X-ray Photoelectron Spectroscopy. The Pt films grown on Si(100) were characterized by X-ray photoelectron spectroscopy (XPS) and Auger electron spectroscopy (AES). The samples were transferred via a vacuum load lock into a KRATOS XSAM 800, equipped with a dual anode (Mg/Al) X-ray source and scanning Auger microprobe (SAM) capabilities. The films were Ar^+ bombarded to expose the region of bulk composition and then characterized. The XPS data were collected with both Al and Mg X-ray sources, and a representative spectrum showing the C 1*s* and O 1*s* regions are shown in Figure 9. The detection limits for XPS and AES are similar and are much better than 1.0 atom % for most elements. The Auger spectra demonstrate that the Pt films are free of impurities such as oxygen and sulfur, although the presence of nearby Pt peaks obscures the C region of the spectrum. For this reason, XPS was the primary technique to determine the C content of the films, which has an upper limit of 1 atom %. This level of contamination is significantly lower than that typically observed from Ar^+-bombarded Pt foils obtained commercially that are nominally 99.99% pure.

Discussion

Physical Properties. The melting points of cyclopentadienyl compounds are found to be significantly higher than those of the corresponding methylcyclopentadienyl analogues, the difference ranging from as little as 41 °C in $(R\text{-}C_5H_4)_2V$ (mp R = H, 67–8 °C; R = Me, 26–8 °C) to as much as 215 °C in $(R\text{-}C_5H_4)_3Nd$ (mp R = H, 380 °C; R = Me, 165 °C).[18] A compilation of these is shown in Supplementary Material Table A. The melting point lowering by substitution of a methyl group for hydrogen on $(R\text{-}C_5H_4)PtMe_3$ is somewhere in the middle of this range, i.e., 79 °C [mp R = H, 108.5 °C;[19] R = Me, 29.5–30.0 °C (this work)].

The vapor pressure of $CpPtMe_3$ was first reported by Egger[19] with the isoteniscope technique. This implies that the experimental values were obtained in the liquid range (above the melting point of $CpPtMe_3$). Adamson et al.[20] later quoted a vapor pressure of 0.052 Torr for $CpPtMe_3$ at 20 °C citing a personal communication from Egger and James. This is somewhat higher than the value determined in the present work (see Experimental Section and Results). As expected, the vapor pressure of **1** is higher than that of $CpPtMe_3$, paralleling the lower melting point in the former.

Solution ^1H and ^{13}C NMR. Only one resonance due to the three methyl groups attached to platinum is seen both in the ^1H and the $\{^1H\}^{13}C$ solution NMR (see Figures 1 and 2) indicating a rapid exchange of the environment of these groups. This is probably brought about by the rotation of the η^5-MeCp ring. The $C_{(ring)}$ resonances are seen as a 1:2:2 pattern in the $\{^1H\}^{13}C$ NMR; in solution different $^{195}Pt\text{–}^{13}C_{(ring)}$ coupling constants are observed. This must be due to some asymmetry in the Pt-ring bonding, i.e., an asymmetry in the *s*-character of the $Pt\text{–}C_{(ring)}$ orbitals. If present, this is *not* reflected in the $Pt\text{–}C_{(ring)}$ bond distances in the solid-state structure (see below). However, this does not preclude the possibility of an asymmetric structure (i.e., η^3-MeCp) in solution.

Table II. Comparison of the Relative Intensities of X-ray Diffraction

	Pt source	reflection relative intensity[a] (%) 200	220	311	222
1	Pt. ref powder	53	31	33	12
2	$CpPtMe_3$/Pyrex[b]	40	14	11	11
3	$CpPtMe_3$/Si(100)[b]	4			7
4	$(MeCp)PtMe_3$/Pyrex	15	6	7	6
5	$(MeCp)PtMe_3$/Si(100)	60		12	7

[a] Relative of *111* reflection = 100%. [b] See ref 8.

Crystallographic Study and Solid-State ^{13}C NMR. The unit cell of **1** does not adopt a crystallographically imposed inversion symmetry (see packing diagram, Figure 4). The methyl groups on platinum are nonequivalent, as are also the individual ring carbon atoms. The solid-state $\{^1H\}^{13}C$ NMR spectra at 288, 200, and 176 K (Figure 3) do indeed show five resonances for the ring carbon atoms. However, only a single resonance at −19 ppm ($J^{195}Pt\text{–}^{13}C$ = 711 Hz) is seen for the methyl groups on platinum at 288 K. This averaged signal is close to that observed in solution (δ = −18.4 ppm, $J^{195}Pt\text{–}^{13}C$ = 716 Hz) and indicates a rapid exchange of the environment of the methyl groups in the solid state. Since rotation of the MeCp ring is not possible in the solid state (see comments above) averaging the environment of the methyl groups bonded to platinum must be brought about by rotation of the $PtMe_3$ groups. At 200 K, the methyl resonances broaden (middle trace, Figure 3), and in the limiting spectrum (176 K, upper trace, Figure 3) the resonance of the $PtMe_3$ groups is seen to be split into three signals by the crystallographically imposed asymmetry (Figure 4).

In the individual molecule, the methylcyclopentadienyl unit is bound to the platinum center in a pentahapto fashion with the platinum carbon distances in the range of 2.260 to 2.354 Å, essentially the same within experimental error. The range of the $Pt\text{–}C_{(ring)}$ distances in $(MeCp)PtMe_3$ is narrower than that in $CpPtMe_3$ (2.19–2.48 Å),[20] while the average value (2.304 Å) is comparable to the average $M\text{–}C_{(ring)}$ distances in $CpW(CO)_3Au(PPh_3)$ (2.36 Å),[21] Cp_2Os, (2.22 Å),[22] and $CpRe(CO)_3$, (2.284 Å).[23]

Deposition and Physical Characterization of the Pt Films. Miller et al.[24] have recently studied the hydrogenation of organometallic complexes catalyzed by platinum black. These parallel our observations of the deposition of platinum on surfaces in the presence of hydrogen. Kinetic studies[25] of the deposition of $CpPtMe_3$ indicate an induction period in the absence of a previously formed metallic film; thus the deposition is surface catalyzed. It is difficult to see how the platinum can contact the surface in the ground state of the molecule (see Figure 5). Thus we believe some dislocation of the η^5-MeCp ring to lower hapticity is required before the platinum atom of the hydrocarbon complex may interact with surface metal atoms.

The deposited films were analyzed by X-ray diffraction, scanning electron microscopy (SEM), and X-ray photoelectron spectroscopy (XPS). The X-ray powder diffraction pattern of a Pt film deposited on silicon shown in Figure 7 contains the same reflections as a standard powder diffraction of polycrystalline platinum metal;[26] the sharp lines indicate a high polycrystallinity for the metal film. However, as shown in Table II, the intensity pattern of the reflections from the thin films differs from those

(18) *Dictionary of Organometallic Compounds*; Buckingham, J., Ed.; Chapman and Hall: New York, 1984; Vol. 1 and 2.
(19) Egger, K. W. *J. Organomet. Chem.* **1970**, *24*, 501–506.
(20) Adamson, G. W.; Bart, J. C. J.; Daly, J. J. *J. Chem. Soc. A* **1971**, 2616–2619.
(21) Wilford, J. B.; Powell, H. M. *J. Chem. Soc. A* **1969**, 8–15.
(22) Jellinek, F. *Z. Naturforsch.* **1959**, *14B*, 737–738.
(23) Fitzpatrick, P. J.; Le Page, Y.; Butler, I. S. *Acta Crystallogr.* **1981**, *B37*, 1052–1058.
(24) (a) Miller, T. M.; Izumi, A. N.; Shih, Y.-S.; Whitesides, G. M. *J. Am. Chem. Soc.* **1988**, *110*, 3146–3156. (b) Miller, T. M.; McCarthy, T. J.; Whitesides, G. M. *J. Am. Chem. Soc.* **1988**, *110*, 3156–3163. (c) Miller, T. M.; Whitesides, G. M. *J. Am. Chem. Soc.* **1988**, *110*, 3164–3170.
(25) Thridandam, H.; Hick, R. F., manuscript in preparation.
(26) Joint Committee on Powder Diffraction Standards. *Powder Diffraction File: Inorganic Phases* (International Center for Diffraction Data, Swarthmore, PA, 1985).

of the standard as well as from those in other deposited films. The closest match in intensity is achieved in the deposits on Pyrex glass (entries nos. 2 and 4, Table II). One may assume little or no preferential orientation in these deposits. The deposition of Pt from (MeCp)$PtMe_3$, **1**, occurs at the lowest temperature (120 °C); these deposits show the greatest departure from the isotropic standard reflections. However, on the Si(100) surfaces there is preferred orientation; the most pronounced is seen in entry no. 5, with the Pt(200) being favored for the surface deposited films. By comparison, Pt films deposited in 3 min from $Pt(ethylene)_3$ at 50 °C in an ethylene stream (<1 atom % C) are amorphous.[27] The film resistivity for the Pt films was found to be around 26 μΩ·cm. This value is somewhat higher than the film resistivity for Pt films derived from $Pt(PF_3)_4$ (18 μΩ·cm),[4] and may be due to the lower temperature of deposition.

Analyses by X-ray photoelectron spectroscopy (XPS, Figure 9) shows no detectable amount of carbon (<1 atom % C) in the bulk of the film. These analyses are carried out after Ar^+ sputtering to remove the oxygen- and carbon-containing impurities on the surface. No other impurities are detected in the platinum. Scanning electron microscopy (SEM, Figure 8) shows smooth film composed of crystallites about 250 Å across compared with 1000 Å across in the Pt film from $CpPtMe_3$.[8]

(27) Müller, H.-J.; Kaesz, H. D., manuscript in preparation.

Acknowledgment. This work was supported in part by a grant from the Raychem Corporation with a matching grant from the University of California Microelectronics Innovation and Computer Research Opportunities (MICRO) Program. We thank H. Thridandam and Dr. H.-J. Müller for permission to quote experimental results prior to publication. We also thank Dr. S. Khan for assistance with XRD studies, H. Thridandam and A. Lee for assistance with the SEM, Dr. Y.-J. Chen for helpful discussions, Yihui Yang and Professor J. S. Valentine for assistance with the UV spectra, and A. Owyeung for assitance with the illustrations.

Registry No. 1, 94442-22-5; MeCp, 26519-91-5; Me_3PtI, 14364-93-3; Pt, 7440-06-4.

Supplementary Material Available: ^1H homonuclear COSY contour plot of (MeCp)$PtMe_3$, **1** (Figure A), ^1H-^{13}C heteronuclear shift correlation contour plot of **1** (Figure B), diagram of the apparatus for the vapor pressure measurement (Figure C), UV spectrum of **1** in heptane (Figure D), least-squares plots of UV absorbance vs concentration of $CpPtMe_3$ and **1** (Figures E and F), comparison of melting points of $(R\text{-}C_5H_4)_nML_x$ (R = H or Me) (Table A), final atomic parameters (Table B), selected bond distances and angles (Tables C and D), and final thermal parameters for the Pt atom (Table E) (8 pages); table of observed and calculated structure factors (4 pages). Ordering information is given on any current masthead page.

Reactions of Carbon Atoms/Clusters with Methane, Methyl Bromide, and Water at 10 and 77 K

Gi Ho Jeong,[‡,1] Kenneth J. Klabunde,*[,‡] Ohm-Guo Pan,[†] G. C. Paul,[†] and Philip B. Shevlin*[,†]

Contribution from the Departments of Chemistry, Kansas State University, Manhattan, Kansas 66506, and Auburn University, Auburn, Alabama 36849. *Received April 3, 1989*

Abstract: The reactions of C atoms, C_2, and C_3 were monitored under matrix isolation conditions (10 K, argon) with methane, methyl bromide, and water. With CH_4 + C, the singlet state (^1D) reacted by C-H insertion followed by rearrangement to ethylene. Ground-state ^3P atoms did not react, although C_2 reacted but products could not be spectroscopically determined. Trimer C_3 and higher clusters did not react with CH_4. With CH_3Br, C, C_2, C_3, and higher clusters all reacted. The main product with C atoms was the stabilized carbene CH_3CBr formed by C-Br insertion. With H_2O, a major product was CO formed from ^1S and/or ^1D carbon atoms. Carbon clusters also reacted, but less efficiently than with CH_3Br. In order to determine the nature of the isolable products when carbon vapor reacted with methane, carbon arc experiments and 5-diazotetrazole decomposition experiments were carried out at 77 K. Isotope labeling and product analyses showed that C_1 reacted both by C-H insertion and hydrogen abstraction, and one mode for acetylene formation may be dimerization of CH. Vapor components C_2 and C_3 react with methane by hydrogen abstraction processes at 77 K.

Reactions of carbon atoms, dimers, and trimers have fascinated scientists for many years.[2] A variety of methods have been employed to generate carbon vapor, including arcs and thermal (resistive) heating. Differing portions of C versus C_2 versus C_3 are found with different evaporation methods.

The chemistry of C, C_2, and C_3 has been studied under a variety of conditions:[3] (a) simultaneous deposition of carbon vapor and reactant on a cold surface; (b) time-delay techniques, in which less than a monolayer of carbon is deposited onto an inert substrate and reactant added later; (c) gas-phase reactions (pyrolysis of reactant is a severe problem); and (d) lasers used to evaporate carbon in pulses; heating proceeds on a much shorter time scale.

Laser evaporation of carbon does provide some advantages.[4] A laser pulse can be very short, and the material evaporated can traverse the distance to the reaction zone (in this case a cold window) in the dark. During this time all excited state species will radiatively decay unless they are metastable states. Thus, in this work we evaporated carbon by focusing a XeCl excimer laser beam on a graphite rod. The experimental setup has been

Table I. Second-Order Rate Constants of C (^3P, ^1D) with Various Gases (k: $cm^3\ s^{-1}$ $molecule^{-1}$)[a]

gas	C(^3P)	C(^1D)
NO	$7.3 \pm 2.2 \times 10^{-11}$	$4.7 \pm 1.3 \times 10^{-11}$
O_2	$3.3 \pm 1.5 \times 10^{-11}$	2.6×10^{-11}
CO	$6.3 \pm 2.7 \times 10^{-32}$	$1.6 \pm 0.6 \times 10^{-11}$
CH_4	$<2.5 \times 10^{-15}$	$2.1 \pm 0.5 \times 10^{-10}$
H_2O	$<3.6 \times 10^{-13}$	1.7×10^{-11}

[a] Data taken from ref 7.

[‡] Kansas State University.
[†] Auburn University.

(1) On leave from the Department of Chemistry, Busan National University, Busan, 609-735 South Korea.

(2) For recent reviews of the chemistry of atomic carbon see: (a) Skell, P. S.; Havel, J.; McGlinchey, M. J. *Acc. Chem. Res.* **1973**, *6*, 97-105. (b) Mackay, C. In *Carbenes*; Moss, R. A., Jones, M., Jr., Eds.; Wiley-Interscience: New York, 1975; Vol. II, pp 1-42. (c) Shevlin, P. B. In *Reactive Intermediates*; Abramovitch, R. A., Ed.; Plenum Press: New York, 1980; Vol. I, pp 1-36.

0002-7863/89/1511-8784$01.50/0